In Vivo Protection Provided by a Synthetic New Alpha-Galactosyl Ceramide Analog against Bacterial and Viral Infections in Murine Models[∇]

Kun-Hsien Lin,[1,2]† Jian-Jong Liang,[3]† Wen-I Huang,[1] Shao-Ying Lin-Chu,[1] Ching-Yao Su,[1,4]
Yi-Ling Lee,[3] Jia-Tsong Jan,[1] Yi-Ling Lin,[1,3]* Yih-Shyun E. Cheng,[1]
and Chi-Huey Wong[1,2,4]*

*Genomics Research Center[1] and Institute of Biomedical Sciences,[3] Academia Sinica, Taipei 115, Taiwan, and Department of
Chemistry[2] and Institute of Biochemical Sciences,[4] National Taiwan University, Taipei 106, Taiwan*

Alpha-galactosyl ceramide (α-GalCer) has been known to bind to the CD1d receptor on dendritic cells and activate invariant natural killer T (iNKT) cells, which subsequently secrete T-helper-cell 1 (Th1) and Th2 cytokines, which correlate with anti-infection activity and the prevention of autoimmune diseases, respectively. α-GalCer elicits the secretion of these two cytokines nonselectively, and thus, its effectiveness is limited by the opposing effects of the Th1 and Th2 cytokines. Reported here is the synthesis of a new α-GalCer analog (compound C34), based on the structure of CD1d, with a 4-(4-fluorophenoxy) phenyl undecanoyl modification of the *N*-acyl moiety of α-GalCer. Using several murine bacterial and viral infection models, we demonstrated that C34 has superior antibacterial and antiviral activities in comparison with those of several other Th1-selective glycolipids and that it is most effective by administering it to mice in a prophylactic manner before or shortly after infection.

Natural killer T (NKT) cells contribute to a variety of immunological processes through the recognition of NKT cell receptors by lipid and glycolipid antigens presented by CD1d molecules (2, 35). CD1d molecules are major histocompatibility complex class I-like proteins and are expressed by most monocytes, macrophages, dendritic cells, and B cells as well as by nonlymphoid cells. CD1d presents glycolipid antigens to CD1d-restricted T cells (or NKT cells), which are implicated in the host innate defense system through the production of T-helper-cell 1 (Th1) and Th2 types of cytokines, such as gamma interferon (IFN-γ) and interleukin-4 (IL-4), respectively (32, 39). The production of Th1 cytokines is shown to correlate with the antitumor, antibacterial, and antiviral effects of glycolipids, while the ability to induce the Th2 cytokines is thought to correlate with the amelioration of certain autoimmune diseases, such as type 1 diabetes (9, 10, 28).

Among the variety of ligands that bind to CD1d, the most well studied one is alpha-galactosyl ceramide (α-GalCer) (7, 17, 30), which is a synthetic, structurally optimized compound of the natural product lead identified from the marine sponge (*Agelas mauritianus*) as agelasphin-9b (24). The synthetic analog (2*S*,3*S*,4*R*)-1-*O*-(α-D-galactopyranosyl)-2-(*N*-hexacosanoylamino)-1,3,4-octadecanetriol was made as KRN7000 at Kirin Brewery, Japan (23), and has generally been referred to as α-GalCer. Mice treated with α-GalCer were

shown to be protected against a variety of infections (13, 15, 16, 22, 33). However, the effectiveness of α-GalCer is limited by the opposing effects of the Th1 and Th2 cytokines induced by this glycolipid. In order to develop selective Th1 or Th2 activators, many α-GalCer analogs were synthesized (1, 3, 5, 8, 12, 14, 21, 34, 36), and their immune-modulating activities were shown to be related to the affinity of binding to CD1d (8). Recent studies using a CD1d array established that the secretion of IFN-γ and IL-4 by NKT cells is determined by the binding of α-GalCer analogs to CD1d (21), and a higher affinity for CD1d would shift the cytokine release profile toward a stronger Th1 response (3, 21).

This report described the synthesis of the 4-(4-fluorophenoxy)phenyl undecanoyl derivative of α-GalCer as a selective Th1 activator. This analog was designed on the basis of the structure of CD1d, where the *N*-acyl group of the glycolipid interacts most favorably with the lipid binding moiety of CD1d (36). Its efficacies for protection against both bacterial and viral infections were compared with those of α-GalCer and several other analogs using murine models of infection. Our study found that among the synthetic α-GalCer analogs tested, compound C34 is the most effective in offering protection against all of the bacterial and viral infection models tested, especially when it is given in a prophylactic manner or shortly after infection.

MATERIALS AND METHODS

Reagents and glycolipid testing agents. All the reagents were commercial reagent grade and were used without further purification, unless otherwise specified. All solvents were anhydrous grade. CH₂Cl₂ and methanol (MeOH) were purchased from Acros. Anhydrous CHCl₃ was purchased from Merck. Molecular sieves (4 Å) for glycosylation were purchased from Acros and activated by flame. Reactions were monitored by analytical thin-layer chromatography (TLC) on Merck silica gel 60 F254 plates and were visualized under UV light (254 nm)

---

* Corresponding author. Mailing address: Genomics Research Center, Academia Sinica, 128 Academia Road, Section 2, Nankang District, Taipei 115, Taiwan. Phone for Chi-Huey Wong: 886-2-2789-9400. Fax: 886-2-2785-3852. E-mail: chwong@gate.sinica.edu.tw. Phone for Yi-Ling Lin: 886-2-2652-3902. Fax: 886-2-2785-8847. E-mail: yll@ibms.sinica.edu.tw.
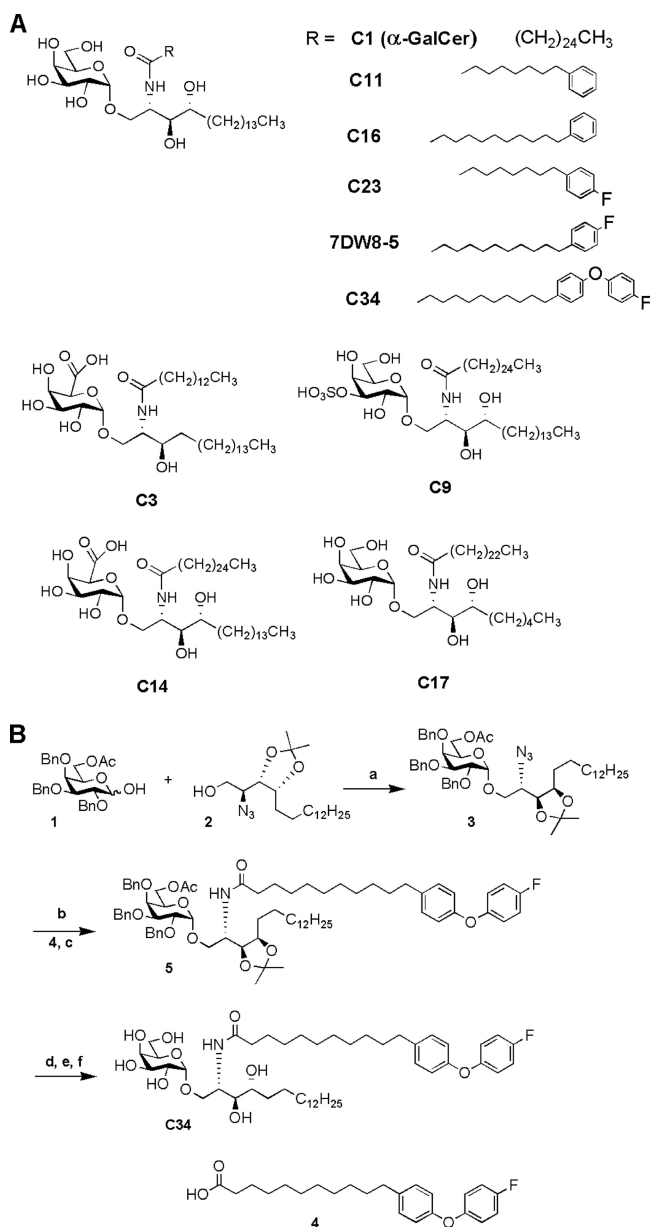
† These authors contributed equally to this work.

FIG. 1. α-GalCer analogs used in the present study. (A) Names and structures of α-GalCer analogs used. (B) Reagents and conditions used for the synthesis of C34 were as follows: a, Me₂S, 2-Cl-pyridine, Tf₂O, CH₂Cl₂, 4-Å molecular sieve, −45°C, 16 h, 60%; b, triphenylphosphine, pyridine, H₂O, 50°C, 9 h; c, 4, EDC, HBTu, Et₃N, CH₂Cl₂, two steps; d, NaOMe, MeOH-CH₂Cl₂ = 1:4, 9 h; e, AcOH-H₂O = 4:1, 70°C, 16 h; f, Pd(OH)₂, H₂, MeOH-CHCl₃ = 4:1, 5 h, 40%, three steps. BnO, benzyl ether; OAc, acetate.

and/or by staining with acidic ceric ammonium molybdate or ninhydrin. Flash column chromatography was performed on a silica gel 60 Geduran column (particle size, 40 to 63 μm; Merck). ¹H nuclear magnetic resonance (NMR) spectra were recorded on a Bruker AV-600 spectrometer (600 MHz) at 20°C. Chemical shifts (δ ppm) were assigned according to the standard signals of CDCl₃ (δ = 7.24 ppm), MeOD (δ = 3.31 ppm), and pyridine-d⁵ (δ = 7.58 ppm). ¹³C NMR spectra were obtained on a Bruker AV-600 spectrometer (150 MHz) and were reported on the δ ppm scale using the signals of CDCl₃ (δ = 77.23 ppm), MeOD (δ = 49.15 ppm), and pyridine-d⁵ (δ = 150.35 ppm) for calibration.

The structures of all glycolipids and their code names used in this study are shown in Fig. 1A. The synthesis and some of the properties of the glycolipids

used in this study were previously reported (3, 8, 21, 36). Compound C34 is a new α-GalCer analog; its synthesis is described in this report (Fig. 1B). Glycolipid stock solutions were prepared as 1-mg/ml dimethyl sulfoxide (DMSO) solutions. The test samples were diluted with phosphate-buffered saline (PBS) to 10 to 30 μg/ml and were used for the animal studies.

Synthetic procedures for compound 3. To a solution of galactosyl donor 1 (5.8 g, 11.8 mmol) (18), dimethyl sulfide (1.1 ml, 15.6 mmol), 4-Å molecular sieve (1 g), and 2-chloropyridine (3.6 ml, 39 mmol) in anhydrous CH₂Cl₂ (30 ml) under Ar at −45°C was added trifluoromethanesulfonic anhydride (2 ml, 11.9 mmol). The reaction mixture was stirred for 20 min at 0°C and 20 min at room temperature. Galactosyl acceptor 2 (6) in CH₂Cl₂ (10 ml) was slowly added, and the reaction mixture was stirred at room temperature for 16 h and then filtered. The organic layer was washed with water and brine, dried over MgSO₄, and concentrated under reduced pressure. The residue was chromatographed on silica gel (ethyl acetate-hexanes [EA-Hex]; 1:20 to 1:15) to give the product (compound 3) as a yellow oil (4 g, 60%). ¹H NMR (600 MHz, CDCl₃) δ 7.37 to 7.24 (m, 15H), 4.95 (d, J = 11.5 Hz, 1H), 4.91 (d, J = 3.6 Hz, 1H), 4.86 (d, J = 11.5 Hz, 1H), 4.77 (d, J = 11.5 Hz, 1H), 4.71 (d, J = 11.5 Hz, 1H), 4.67 (d, J = 11.5 Hz, 1H), 4.59 (d, J = 11.5 Hz, 1H), 4.11 (dd, J = 10.7 Hz, 7.6 Hz, 1H), 4.08 (m, J = 4.4 Hz, 1H), 4.05 (dd, J = 10.1 Hz, 3.6 Hz, 1H), 4.02 (dd, J = 10.7 Hz, 3.5 Hz, 1H), 4.01(dd, J = 10.5 Hz, 2.4 Hz, 1H), 4.00 (dd, J = 9.2 Hz, 4.4 Hz, 1H), 3.95 (dd, J = 10.1 Hz, 2.7 Hz, 1H), 3.92 (dd, J = 7.6 Hz, 3.5 Hz, 1H), 3.83 (d, J = 2.7 Hz, 1H), 3.69 (dd, J = 10.5 Hz, 6.6 Hz, 1H), 3.40 (ddd, J = 9.2 Hz, 6.6 Hz, 2.4 Hz, 1H), 1.95 (s, 3H), 1.60 (m, 1H), 1.50 (m, 1H), 1.35 (s, 3H), 1.34 to 1.20 (m, 27H), 0.85 (t, J = 6.8 Hz, 3H). ¹³C NMR (150 MHz, CDCl₃) δ 170.79, 138.95 × 2, 138.37, 128.67 × 2, 128.58 × 2, 128.55 × 2, 128.47 × 2, 128.00, 127.83 × 2, 127.80 × 2, 127.74, 127.70, 108.39, 98.96, 78.77, 77.93, 76.71, 75.46, 75.02, 74.73, 73.83, 73.15, 69.83, 69.13, 63.91, 59.93, 32.13, 29.90 × 3, 29.87 × 2, 29.83, 29.81, 29.77, 29.57, 29.52, 28.40, 26.73, 25.91, 22.90, 21.03, 14.34. High-resolution mass spectrometry (HRMS; electrospray ionization–time of flight [ESI-TOF]) for C₅₀H₇₁N₃O₉Na⁺ [M + Na]⁺: calculated, 880.5083; found, 880.5064.

Synthesis of compound 4. (10-Carboxynonyl)triphenylphosphonium bromide (4.8 g, 19.1 mmol) (29) was dissolved in 186 ml of tetrahydrofuran (THF). The solution was cooled to 0 to 5°C and was added dropwise to a solution of lithium bis(trimethylsilyl)amide (LHMDS; 1 M in THF-ethylbenzene, 38 mmol) to produce an orange ylide within 1 h at 0 to 5°C. 4-(4-Fluorophenoxy)benzaldehyde (2 g, 9.25 mmol), dissolved in 18 ml of THF, was added dropwise, and the solution was stirred for 4 h at room temperature. Afterwards, the reaction was quenched with methanol and concentrated. The residue was extracted with diethyl ether, water, and brine and then dried over MgSO₄. After removal of the solvent, the mixture was chromatographed on silica gel (EA-Hex, 1:5 to 1:2) to give the unsaturated fatty acid.

The saturated fatty acid was prepared by catalytic hydrogenation in 50 ml of methanol containing 10 mol% of 10% palladium on charcoal (Pd/C). The reaction mixture was stirred under H₂ (1 atm) at room temperature for 1 day. The hydrogenated product was filtered through Celite 545 to remove the catalyst. The resulting solution was concentrated and chromatographed on silica gel (EA-Hex, 1:4 to 1:2) to give the product (compound 4) as a yellow solid (2 g, 58%, two steps). ¹H NMR (600 MHz, MeOD) δ 7.16 (m, 2H), 7.06 (m, 2H), 6.96 (m, 2H), 6.87 (m, 2H), 2.59 (t, J = 7.6 Hz, 2H), 2.27 (m, J = 7.6 Hz, 2H), 1.59 (m, 4H), 1.32 (m, 12H). ¹³C NMR (150 MHz, MeOD) δ 177.97, 160.92, 159.33, 156.94, 155.19, 139.34, 130.88 × 2, 121.27, 121.22, 119.61 × 2, 117.34, 117.19, 36.24, 35.11, 32.93, 30.72, 30.66 × 2, 30.50, 30.36, 26.21. HRMS (ESI-TOF) for C₂₃H₂₉FO₃Na⁺ [M + Na]⁺: calculated, 395.1993; found, 395.1998.

Synthesis of compound 5. To a solution of compound 3 (4 g, 4.7 mmol) in pyridine-H₂O (10:1, 187 ml) was added triphenylphosphine (2.5 g, 9.4 mmol). The mixture was stirred for 16 h at 45°C, concentrated, dissolved with ethyl acetate, washed with brine, and concentrated again to dryness. The residue was used for the next step without prior purification.

To a stirred solution of this compound, fatty acid 4 (2.1 g, 5.6 mmol) in 36 ml of anhydrous CH₂Cl₂ (36 ml) was added, along with triethylamine (Et₃N; 1.3 ml), 1-ethyl-3-(3-dimethylaminopropyl)carbodiimide hydrochloride (EDC; 1.3 g, 7.1 mmol), and O-benzotriazole-N,N,N′,N′-tetramethyl-uronium-hexafluoro-phosphate (HBTu; 2.7 g, 7.1 mmol). The solution was stirred for 16 h at ambient temperature and was extracted sequentially with CH₂Cl₂, water, and brine and then dried over MgSO₄. The mixture was concentrated and chromatographed on silica gel (EA-Hex, 1:10 to 1:5) to give the product (compound 5) as a white solid (4.8 g, 88%, two steps). ¹H NMR (600 MHz, CDCl₃) δ 7.40 to 7.23 (m, 15H), 7.10 (d, J = 8.4 Hz, 2H), 6.99 (t, J = 8.8 Hz, 2H), 6.92 (m, 2H), 6.85 (d, J = 8.4 Hz, 2H), 6.01 (d, J = 9.2 Hz, 1H), 4.99 (d, J = 3.6 Hz, 1H), 4.94 (d, J = 11.5 Hz, 1H), 4.81 (d, J = 11.5 Hz, 1H), 4.79 (d, J = 11.5 Hz, 1H), 4.76 (d, J = 11.5 Hz, 1H), 4.66 (d, J = 11.5 Hz, 1H), 4.60 (d, J = 11.5 Hz, 1H), 4.14 to 4.02 (m, J = 3.6 Hz, 5H), 3.97 (m, 1H), 3.90 to 3.86 (m, J = 2.6 Hz, 2.5 Hz, 3H), 3.84 (dd, J = 11.1

Hz, 2.6 Hz, 1H), 3.62 (dd, $J = 11.1$ Hz, 2.5 Hz, 1H), 2.54 (t, $J = 7.7$ Hz, 2H), 2.08 to 1.98 (m, 2H), 1.97 (s, 3H), 1.60 to 1.50 (m, 1H), 1.47 (m, 1H), 1.40 (s, 3H), 1.36 (m, 1H), 1.30 (s, 3H), 1.29 to 1.19 (m, 39H), 0.85 (t, $J = 6.7$ Hz, 3H). ^{13}C NMR (150 MHz, CDCl$_3$) δ 172.54, 170.83, 159.60, 158.00, 158.58, 153.57, 138.67, 138.43, 138.26, 138.06, 129.77 × 2, 128.67 × 2, 128.65 × 2, 128.60 × 2, 128.58 × 2, 128.19 × 2, 128.12, 128.09, 127.92, 127.72 × 2, 120.30, 120.25, 118.54 × 2, 116.44, 116.29, 108.12, 98.85, 79.08, 77.98, 76.86, 75.86, 74.79, 74.57, 73.80, 73.22, 69.07, 68.80, 64.03, 48.72, 37.04, 35.41, 32.14, 31.86, 29.93 × 4, 29.88 × 2, 29.85 × 2, 29.79, 29.76, 29.67, 29.58 × 2, 29.54, 29.07, 28.34, 26.80, 26.12, 25.90, 22.90, 21.03, 14.34. HRMS (matrix-assisted laser desorption ionization–time of flight) for C$_{73}$H$_{100}$FNO$_{11}$Na$^+$ [M + Na]$^+$: calculated, 1,208.7173; found, 1,208.7135.

Synthesis of compound C34. To a solution of 5 (4.8 g, 4 mmol) in cosolvent MeOH-CH$_2$Cl$_2$ (4:1, 50 ml) was added sodium methoxide (NaOMe; 0.4 mmol). The solution was stirred overnight at room temperature. The mixture was neutralized with Amberlite IR-120 resin and then filtered. The solution was concentrated and used for the next step without prior purification.

The solution in acetyl hydroxide (AcOH)-H$_2$O (4:1, 50 ml) was stirred for 16 h at 70°C and was concentrated to dryness. The residue was purified by flash column chromatography on silica gel (EA-Hex-MeOH, 1:1:0.1).

The deacetonide derivative was dissolved in 50 ml of cosolvent MeOH-CHCl$_3$ (4:1, 50 ml) containing palladium hydroxide on carbon (20% Pd, trace), and the mixture was stirred at room temperature for 1 day in an H$_2$ atmosphere. The hydrogenated product was filtered through Celite 545 to remove the catalyst, and the filtrate was concentrated to dryness. The residue was eluted from LH20 (MeOH-CHCl$_3$, 1:1) to give compound C34 (1.3 g, 40%, three steps). ^{1}H NMR (600 MHz, pyridine-d^5) δ 8.53 (d, $J = 8.6$ Hz, 1H), 7.27 (d, $J = 8.4$ Hz, 2H), 7.14 (t, $J = 8.4$ Hz, 2H), 7.05 to 7.09 (m, 4H), 5.59 (d, $J = 3.8$ Hz, 1H), 5.27 (m, 1H), 4.70 to 4.65 (m, 2H), 4.55 (d, $J = 2.6$ Hz, 1H), 4.52 (t, $J = 6.0$ Hz, 1H), 4.45 to 4.39 (m, 4H), 4.35 to 4.30 (m, 1H), 2.59 (t, $J = 7.6$ Hz, 2H), 2.45 (t, 2H), 2.30 (m, 1H), 1.91 (m, 2H), 1.81 (m, 2H), 1.68 (m, 2H), 1.59 (m, 2H), 1.47 to 1.15 (m, 40H), 0.87 (t, $J = 6.9$ Hz, 3H). ^{13}C NMR (150 MHz, pyridine-d^5) δ 173.79, 160.19, 158.60, 156.32, 154.53, 138.89, 130.73 × 2, 121.06, 121.01, 119.46 × 2, 117.25, 117.09, 102.00, 77.17, 73.53, 72.96, 72.09, 71.46, 71.29, 70.79, 69.07, 63.12, 51.95, 37.27, 35.86, 34.82, 32.60, 32.47, 30.84, 30.63, 30.48 × 3, 30.41, 30.35, 30.28, 30.25 × 2, 30.20, 30.10, 30.03, 29.99, 26.87, 23.42, 14.77. HRMS (ESI-TOF) for C$_{47}$H$_{76}$FNO$_{10}$Na$^+$ [M + Na]$^+$: calculated, 856.5345; found, 856.5362.

Mice, viruses, and bacteria used. C57BL/6 and BALB/c mice at 6 to 8 weeks of age were used for the studies. Mice were housed in plastic cages with free access to food and water and were allowed to acclimate at least 1 week prior to the start of the experiments. The viruses used in this study are influenza virus strain WSN (A/WSN/1933/H1N1) and Japanese encephalitis virus (JEV; strain RP-9), as described previously (20, 27). The bacterial strain *Sphingomonas capsulata* (ATCC 14666) was obtained from BCRC, Taiwan. Luminescent strain *Staphylococcus aureus* Xen29 (19) was purchased from Xenogen Corporation (CA). The mouse experiments were approved and performed in accordance with the guidelines of the Academia Sinica Institutional Animal Care and Utilization Committee. The immunodeficient mice used in this study are as described previously (20).

Antibacterial efficacy study using *Sphingomonas capsulata*-infected mice. Six-to-eight-week old female C57BL/6 mice were injected intraperitoneally (i.p.) with 5×10^8 *Sphingomonas capsulata* organisms. The mice were grouped into treatment and control groups at 5 to 10 mice per group. Three hours after the infection, the mice in the treatment group were injected intraperitoneally with the test glycolipids at 50 or 100 µg/kg of body weight, and the mice in the control group were injected with the same volume of PBS. Twenty-four hours after bacterial infection, mice from all groups were killed. The livers were removed and homogenized in 0.9% NaCl with 0.02% Tween 80 using tissue homogenizers. The numbers of CFU of *Sphingomonas capsulata* in the liver homogenates were determined by plating diluted samples on nutrient plates. Colonies were counted after incubation for 48 h at 37°C. The antibacterial results were analyzed using a one-way analysis of variance (ANOVA) to assess the significance of the difference between treatment groups, followed by the Tukey posttest.

Antibacterial efficacy study using luminescent *Staphylococcus aureus* (Xen29) by image analyses. BALB/c female mice were weighed, grouped, and injected in the posterior quadricep muscle of the left thigh with 200 µl PBS containing 3×10^8 CFU of *S. aureus* Xen29. At different times after Xen29 infection, the mice were injected i.p. with vehicle or glycolipid, as indicated. Mice were periodically imaged using an IVIS *in vivo* imaging system (Xenogen Corporation), as described previously (19). The imaging results, in relative luminescence units, were analyzed using one-way ANOVA to assess the significance of the difference between treatment groups, followed by the Tukey posttest.

JEV infection animal model. Seven-week-old C57BL/6 mice were grouped, and at various times postinfection the JEV-infected mice received glycolipids.
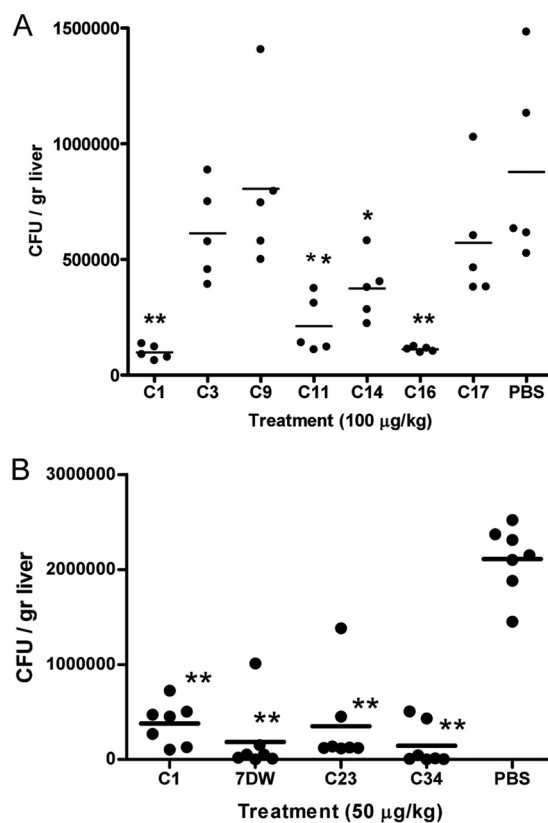

FIG. 2. Antibacterial efficacies of glycolipids in mice infected with *Sphingomonas capsulata*. (A) Infected mice were grouped and received 100 µg/kg α-GalCer analogs or vehicle control. They were killed at 24 h postinfection to determine the liver bacterial loads, which are represented by dots. The mean numbers of CFU of each treatment group are indicated with short horizontal lines. (B) An experiment similar to that described for panel A was conducted by administering 50 µg/kg of selected glycolipids to different groups of mice. Asterisks indicate groups with results significantly different from those for the PBS-treated control group: ∗, $P < 0.05$; ∗∗, $P < 0.01$.

The infection was done by i.p. injection of 5×10^5 PFU of the RP-9 strain of JEV in 500 µl PBS, and 30 µl PBS was simultaneously injected intracerebrally, as described previously (4, 20, 38). The survival of the mice was monitored daily. The survival curves for the glycolipid-treated groups were compared to those for the control group using Prism software (GraphPad Software, San Diego, CA).

Anti-influenza animal model study. For the evaluation of the *in vivo* anti-influenza efficacies of the α-GalCer analogs, BALB/c mice were treated with C34 at different times after nasal infection using 10 50% lethal doses (LD$_{50}$s) of strain WSN influenza virus. The survival of the mice in all groups was examined daily for 14 days postinfection. The survival curves for the glycolipid-treated groups were compared to those for the control group using Prism software (GraphPad Software).

RESULTS AND DISCUSSION

Synthesis of the new α-GalCer analog C34. The structures of all glycolipids and their code names used in this study are shown in Fig. 1A. Compounds C1, C3, C9, C11, C14, C16, C17, C23, and 7DW8-5 were prepared as described previously (3, 8, 21, 36). As shown in Fig. 1B, the synthesis of C34 involved the coupling of the galactosyl donor (compound 1) with phytosphingosine (compound 2) using trifluoromethanesulfonic anhydride (Tf$_2$O) and dimethyl sulfide (Me$_2$S) as the promoter afforded compound 3 at a 60% yield. The α/β selectivity was
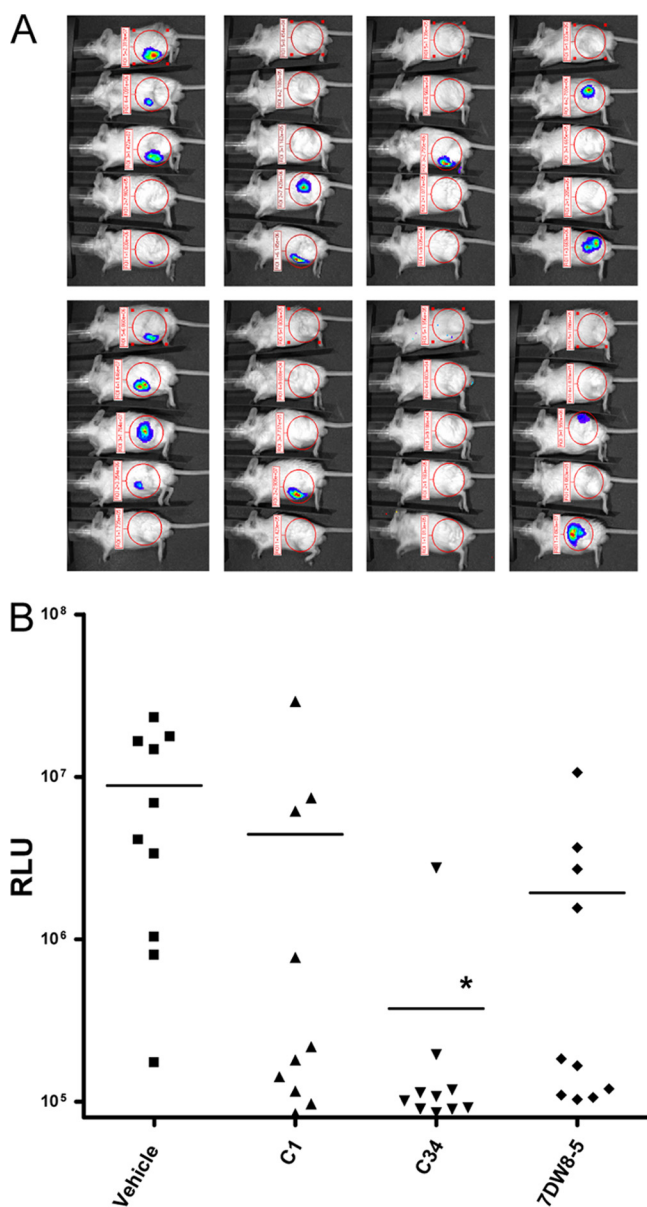
FIG. 3. Antibacterial efficacies of selected glycolipids in the *Staphylococcus aureus* thigh infection model. The antibacterial efficacies of glycolipids (150 μg/kg) that were administered by i.p. injection at 3 h postinfection were evaluated by image analyses of luminescent *S. aureus* Xen29. (A) Images of mice in different treatment groups taken 48 h after infection. (B) The relative luminescence unit (RLU) values of each mouse measured 48 h after infection were plotted as individual symbols, and the mean values for the treatment groups are shown with horizontal lines. ∗, $P < 0.05$.

increased when the acetyl protecting group was at the 6 position of the galactosyl donor (compound 1). The azide (compound 3) was reduced using the Staudinger reaction, and the resulting amine was coupled with fatty acid (compound 4) to give compound 5 at an 88% yield. Finally, the protecting groups of compound 5 were removed by several reactions, resulting in C34 at a 40% yield in three steps.

Antibacterial efficacy of α-GalCer analogs in *Sphingomonas capsulata*-infected mice. The *Sphingomonas capsulata*-infected

mice were used as the infection model to evaluate the antibacterial efficacies of some of the synthetic glycolipids. *S. capsulata* is a common environmental bacterial strain that is found in many places, such as air and water. It can easily be identified on nutrient agar plates because of its yellow colony color. Unlike most Gram-negative bacteria, *S. capsulata* does not contain lipopolysaccharide (LPS), which activates the host antibacterial activities. The antibacterial activities of glycolipids in *S. capsulata* are mediated through the activation of NKT cells by glycolipid-bound CD1d molecules; thus, the antibacterial efficacies reflect the impact of the NKT cell-mediated pathway. Figure 2A shows that mice in the treatment groups receiving 100 μg/kg of compound C1, C11, C14, or C16 had significantly lower *S. capsulata* CFU numbers in the livers than the control group at 24 h after bacterial infection. In contrast, the reduction in the numbers of CFU in the groups treated with compounds C3, C9, and C17 were not significantly different from the numbers of CFU found in the control group. The result of this study suggested that the glycolipids α-GalCer (compound C1) and C16 appeared to be more potent than compounds C11 and C14 at suppressing *S. capsulata in vivo*, though the differences are not significant.

The *S. capsulata*-infected mice were then used to compare the antibacterial potency of α-GalCer with the potencies of compound C34 and other analogs, such as compounds C23 and 7DW8-5, that induce high levels of Th1 cytokine secretion (21). These glycolipids were evaluated at 50 μg/kg using the *S. capsulata*-infected C57BL/6 mouse model. Figure 2B shows that treatments with any one of the three glycolipids (compound C34, C23, or 7DW8-5) reduced the bacterial loads significantly compared with the loads in the vehicle-treated mice, with *P* values being less than 0.01. The mean number of CFU for the C34-treated mice appeared to be lower than that for the α-GalCer-treated group. The present study further confirmed that glycolipids biased toward the Th1 pathway are more effective as antibacterial agents than compound C1. However, differences between these glycolipid-treated groups were not significant in the present study.

Antibacterial activities of α-GalCer analogs in the thigh wound mouse model using luminescent *Staphylococcus aureus* (Xen29). As shown above, intraperitoneal injection of C57BL/6 mice with *S. capsulata* results in transient infections, and treatment with some glycolipids hastens the clearance in the 24 h after infection. However, in the absence of any treatment, the infections are often cleared in 2 to 3 days. To evaluate the antibacterial efficacies of the α-GalCer analogs, we then used a more relevant disease model, the mouse model of deep thigh wound infection, by infection of mice in the hind thigh muscle with luminescent *S. aureus* Xen29. The *S. aureus* Xen29 infection can be monitored by image analyses of live mice, which show the reductions in the numbers of CFU in the experimental mice and allows repeated examination of the infections without the need to sacrifice the mice prior to the end of the study. Figure 3 shows that treatment of the thigh muscle-infected mice with compounds α-GalCer and 7DW8-5 3 h after infection resulted in increased clearance for many treated mice; however, a statistically significant difference ($P < 0.05$) in comparison to the clearance for the vehicle-treated group was noted only for the group receiving C34. This result
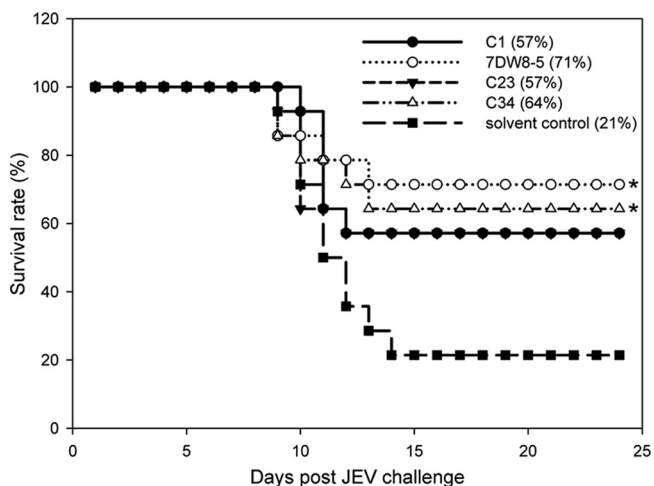
FIG. 4. Glycolipids enhance host protection against JEV infection. Seven-week-old C57BL/6 mice were injected i.p. with 1 μg of compound C1, 7DW8-5, C23, or C34 1 day before virus challenge. The mice were infected i.p. with 5×10^5 PFU of JEV (RP-9 strain) and simultaneously injected intracerebrally with 30 μl PBS. One day after viral infection, the mice were boosted i.p. with 1 μg of compound C1, 7DW8-5, C23, or C34 or with solvent. The mice were monitored daily for 25 days, and the percent of survival is shown. Fourteen mice were included in each experimental group. Survival curve comparisons were performed by statistical analysis by the log rank test using Prism software, and a P value of <0.05 for the result for the treated mice compared to the result for the solvent-treated control mice is indicated (∗).

suggests that C34 treatment may have a higher probability of being beneficial for bacterial clearance in this disease model.

Antiviral evaluation of α-GalCer analogs using the JEV infection animal model. To determine whether the glycolipids elicit protective immunity against viral infection, we used a two-dose protocol in which glycolipid was given 1 day before and 1 day after JEV challenge of mice. As shown in Fig. 4, compounds C1 and C23 increased the rate of mouse survival from 21% to 57% by comparison with the rate for the solvent-treated control group. Furthermore, the protective effects were even more profound in mice receiving compounds C34 and 7DW8-5, with the survival rates being 64% and 71%, respectively (Fig. 4). These results suggest that glycolipid-stimulated NKT cells likely contribute to the host defense against JEV infection. Similarly, C34, which is effective in protecting against JEV infections, was also found to prolong the survival of influenza virus-infected BALB/c mice (see below). To further dissect the requirement for the glycolipid-mediated immune protection, we tested whether the beneficial effects of C34 and 7DW8-5 were still noted in mice deficient in the gene for signal transducer and activator of transcription 1 (Stat-1), Ig μ chain, or CD8 α chain. Our studies showed that the protective activity offered by either C34 or 7DW8-5 in wild-type C57BL/6 mice was not demonstrated in immune-deficient mice. Apparently, both the innate and adaptive immune components are required to trigger protective immunity against JEV infection by these glycolipids, as no beneficial effect was noted in mice lacking the gene for Stat-1, the immunoglobulin μ chain, or the CD8 α chain (Fig. 5).
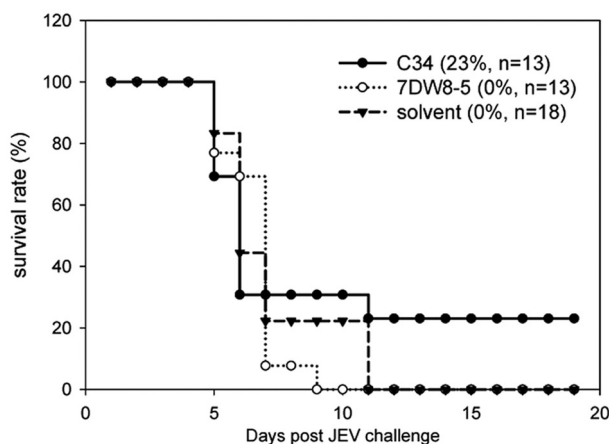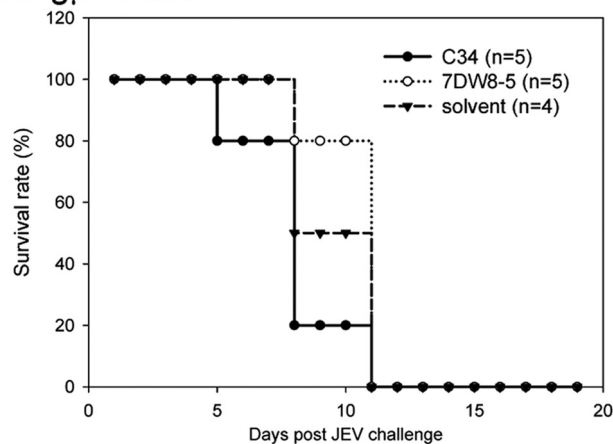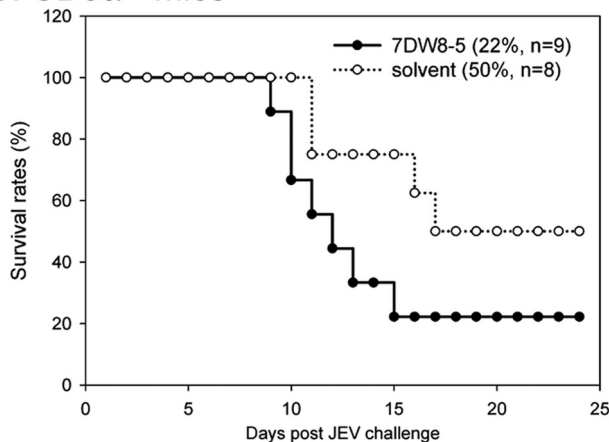

FIG. 5. Glycolipids require host innate and adapted immunity components to trigger protection against JEV infection. Seven-week-old immunodeficient mice lacking Stat-1 (A), immunoglobulin μ chain (B), or CD8 α chain (C) were administered compound C34 or 7DW8-5 or solvent, as described in the legend to Fig. 4, using a two-dose protocol. The Stat-1-knockout mice were intraperitoneally challenged with 0.1 PFU of JEV (RP-9 strain). The Ig μ chain-knockout and CD8 α chain-knockout mice were challenged as described in the legend to Fig. 4. The mice were monitored daily for 25 days. The percent survival is shown, and the number of mice in each experimental group is shown in the key to each panel.
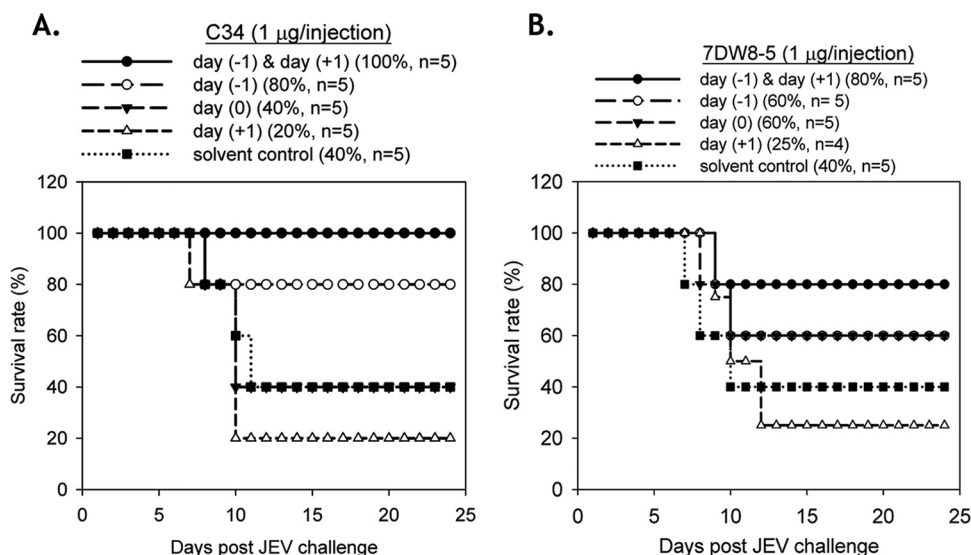
FIG. 6. A two-dose protocol, with doses being administered 1 day before and 1 day after JEV infection, gives the best protective effect. Glycolipid C34 (A) or 7DW8-5 (B) was administered to 7-week-old C57BL/6 mice by a two-dose protocol, as described in the legend to Fig. 4 [day (−1) & day (+1)] or only once 1 day before [day (−1)], on the same day [day (0)], or 1 day after [day (+1)] viral infection. The mice were challenged and monitored as described in the legend to Fig. 4. The percent survival and the number of mice in each experimental group are shown in the key above each panel.

The protective activities of α-GalCer analogs are most effective when it is administered in a prophylactic manner. We assessed whether these glycolipids could generate protective immunity if they were administered after viral infection. Besides the two-dose protocol described above, several one-dose protocols were also tested. In comparison to the two-dose protocol, C34 administered only once on the day before infection elicited a weaker protective effect against JEV. However, if the glycolipids were given once either at the time of infection or 1 day after viral infection, no protection against JEV challenge could be noted (Fig. 6A), suggesting that glycolipid-mediated immune modulation against infection is a time-dependent event. Reduced protective effects were also noted when one dose of compound 7DW8-5 was administered to mice 1 day before JEV infection. When the one dose was given 1 day after infection, no protective effects were found (Fig. 6B). The effects of C34 administration times versus viral infection time were also evaluated in influenza virus (strain WSN)-infected BALB/c mice. Administration of C34 1 day before WSN infection was the most beneficial to mouse survival ($P < 0.01$). Treatment with two doses of C34 administered both 1 day before and 1 day after WSN infection could also significantly prolong survival ($P < 0.05$) so that it was longer than that for the vehicle-treated group. Similar to JEV infection, a single dose of C34 given 1 day after influenza virus infection was not beneficial for survival (Fig. 7). We also studied the effects of the C34 administration times on bacterial clearance using the *S. aureus* thigh infection model. When mouse infections were examined 48 h after infection, bacterial clearance was most profound in the group of mice administered C34 immediately after the thigh infections were introduced. For the group receiving C34 6 h after thigh infection, an improvement in bacterial clearance was noted, but to a lesser extent than that
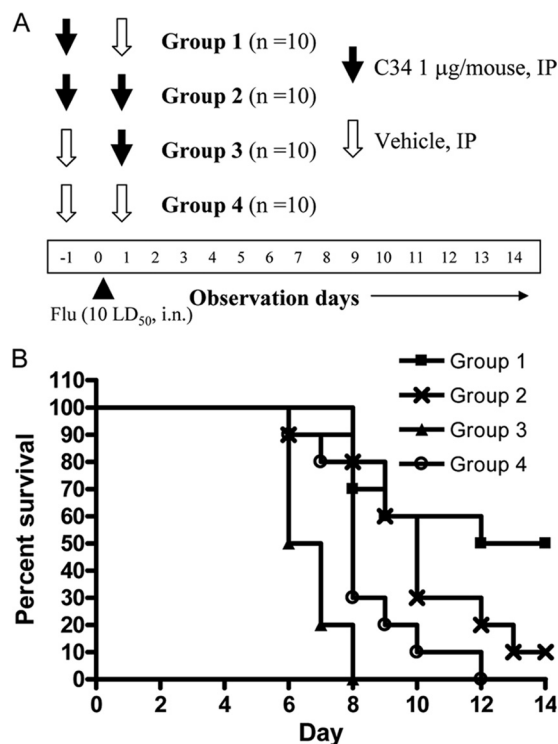

FIG. 7. Survival profile of influenza virus-infected mice receiving compound C34 at different times and different doses. BALB/c mice were infected with 10 LD_{50}s influenza virus WSN by the intranasal (i.n.) route. Mice were grouped into four groups receiving two i.p. injections on both day −1 and day +1 relative to the time of influenza virus infection. (A) Study protocol describing the contents of the i.p. injections (1 μg/mouse C34 or PBS vehicle) and the injection times of the different treatment groups are shown. (B) Survival curves for the different treatment groups.
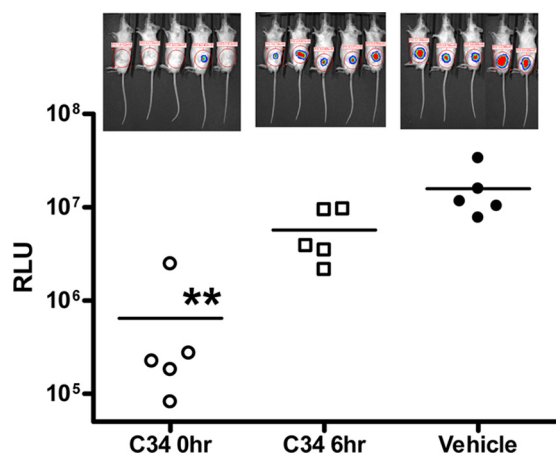
FIG. 8. Effects of time of C34 administration on clearance of infection in the murine thigh wound infection model. Mice infected in the left thigh with luminescent *S. aureus* were grouped into vehicle control group and two treatment groups, which received 150 μg/kg C34 at 0 and 6 h after infection, respectively. Mice were imaged at 48 h postinfection. The images of the luminescent bacterial infection and the relative luminescence units (RLU) are shown as in Fig. 3. **, significant, with *P* being <0.01.

for mice receiving C34 immediately after the thigh infection (Fig. 8).

In the present study, we used murine models of both bacterial and viral infections to evaluate the infection suppression efficacies of several α-GalCer analogs and found that compound C34 is the most efficacious in all models. Previous studies showed that α-GalCer treatment of mice was complicated by its association with detrimental side effects and that treatment efficacy was influenced by a variety of parameters (37). NKT cells respond to infection-associated glycolipids and are stimulated by cytokines produced in dendritic cells upon infection (31). Thus, encountered with glycolipid administration and infection challenges, the immune systems of the experimental mice may experience complicated stimulations. Different cytokine responses were documented in the influenza virus-infected mice, α-GalCer-treated mice, or both influenza virus-infected and α-GalCer-treated mice. Greater serum cytokine levels were often found in the doubly stimulated mice. However, the profiles are complicated and varied at different observation times (11).

The efficacy of α-GalCer for offering protection against LPS-induced shock was found to be dependent on the time of administration, and the glycolipid needs to be administered before or within 2 h after LPS challenge (25, 26). Our *in vivo* studies using bacterial and viral infection models also suggest that compound C34 is the most effective at suppressing infections when it is administered before or shortly after infection. Infections by different microorganisms could result in varied immune stimulations with different kinetics. Thus, for effective protection against infections, both the doses and the numbers of administrations need to be fine-tuned to be beneficial.

REFERENCES

1. **Blauvelt, M. L., M. Khalili, W. Jaung, J. Paulsen, A. C. Anderson, S. B. Wilson, and A. R. Howell.** 2008. Alpha-S-GalCer: synthesis and evaluation for iNKT cell stimulation. Bioorg. Med. Chem. Lett. **18:**6374–6376.
2. **Brigl, M., P. van den Elzen, X. Chen, J. H. Meyers, D. Wu, C. H. Wong, F. Reddington, P. A. Illarianov, G. S. Besra, M. B. Brenner, and J. E. Gumperz.** 2006. Conserved and heterogeneous lipid antigen specificities of CD1d-restricted NKT cell receptors. J. Immunol. **176:**3625–3634.
3. **Chang, Y. J., J. R. Huang, Y. C. Tsai, J. T. Hung, D. Wu, M. Fujio, C. H. Wong, and A. L. Yu.** 2007. Potent immune-modulating and anticancer effects of NKT cell stimulatory glycolipids. Proc. Natl. Acad. Sci. U. S. A. **104:**10299–10304.
4. **Chen, L. K., Y. L. Lin, C. L. Liao, C. G. Lin, Y. L. Huang, C. T. Yeh, S. C. Lai, J. T. Jan, and C. Chin.** 1996. Generation and characterization of organtropism mutants of Japanese encephalitis virus in vivo and in vitro. Virology **223:**79–88.
5. **Chiba, A., S. Oki, K. Miyamoto, H. Hashimoto, T. Yamamura, and S. Miyake.** 2004. Suppression of collagen-induced arthritis by natural killer T cell activation with OCH, a sphingosine-truncated analog of alpha-galactosylceramide. Arthritis Rheum. **50:**305–313.
6. **Fan, G., Y. S. Pan, K. C. Lu, Y. P. Cheng, W. C. Lin, S. Lin, C. H. Lin, C. H. Wong, J. M. Fang, and C. C. Lin.** 2005. Synthesis of α-galactosyl ceramide and the related glycolipids for evaluation of their activities on mouse splenocytes. Tetrahedron **61:**1855–1862.
7. **Franck, R. W., and M. Tsuji.** 2006. Alpha-c-galactosylceramides: synthesis and immunology. Acc. Chem. Res. **39:**692–701.
8. **Fujio, M., D. Wu, R. Garcia-Navarro, D. D. Ho, M. Tsuji, and C. H. Wong.** 2006. Structure-based discovery of glycolipids for CD1d-mediated NKT cell activation: tuning the adjuvant versus immunosuppression activity. J. Am. Chem. Soc. **128:**9022–9023.
9. **Godfrey, D. I., H. R. MacDonald, M. Kronenberg, M. J. Smyth, and L. Van Kaer.** 2004. NKT cells: what's in a name? Nat. Rev. Immunol. **4:**231–237.
10. **Gonzalez-Aseguinolaza, G., L. Van Kaer, C. C. Bergmann, J. M. Wilson, J. Schmieg, M. Kronenberg, T. Nakayama, M. Taniguchi, Y. Koezuka, and M. Tsuji.** 2002. Natural killer T cell ligand alpha-galactosylceramide enhances protective immunity induced by malaria vaccines. J. Exp. Med. **195:**617–624.
11. **Ho, L. P., L. Denney, K. Luhn, D. Teoh, C. Clelland, and A. J. McMichael.** 2008. Activation of invariant NKT cells enhances the innate immune response and improves the disease course in influenza A virus infection. Eur. J. Immunol. **38:**1913–1922.
12. **Hung, L. C., C. C. Lin, S. K. Hung, B. C. Wu, M. D. Jan, S. H. Liou, and S. L. Fu.** 2007. A synthetic analog of alpha-galactosylceramide induces macrophage activation via the TLR4-signaling pathways. Biochem. Pharmacol. **73:**1957–1970.
13. **Johnson, T. R., S. Hong, L. Van Kaer, Y. Koezuka, and B. S. Graham.** 2002. NK T cells contribute to expansion of CD8(+) T cells and amplification of antiviral immune responses to respiratory syncytial virus. J. Virol. **76:**4294–4303.
14. **Kaieda, S., C. Tomi, S. Oki, T. Yamamura, and S. Miyake.** 2007. Activation of invariant natural killer T cells by synthetic glycolipid ligands suppresses autoantibody-induced arthritis. Arthritis Rheum. **56:**1836–1845.
15. **Kakimi, K., L. G. Guidotti, Y. Koezuka, and F. V. Chisari.** 2000. Natural killer T cell activation inhibits hepatitis B virus replication in vivo. J. Exp. Med. **192:**921–930.
16. **Kinjo, Y., D. Wu, G. Kim, G. W. Xing, M. A. Poles, D. D. Ho, M. Tsuji, K. Kawahara, C. H. Wong, and M. Kronenberg.** 2005. Recognition of bacterial glycosphingolipids by natural killer T cells. Nature **434:**520–525.
17. **Kobayashi, E., K. Motoki, T. Uchida, H. Fukushima, and Y. Koezuka.** 1995. KRN7000, a novel immunomodulator, and its antitumor activities. Oncol. Res. **7:**529–534.
18. **Koto, S., N. Morishima, K. Takenaka, K. Kanemitsu, N. Shimoura, M. Kase, S. Kojiro, T. Nakamura, T. Kawase, and S. Zen.** 1989. 2-Methoxyethyl group for protection of reducing hydroxyl group of aldose. Bull. Chem. Soc. Jpn. **62:**3549–3566.
19. **Kuklin, N. A., G. D. Pancari, T. W. Tobery, L. Cope, J. Jackson, C. Gill, K. Overbye, K. P. Francis, J. Yu, D. Montgomery, A. S. Anderson, W. McClements, and K. U. Jansen.** 2003. Real-time monitoring of bacterial infection in vivo: development of bioluminescent staphylococcal foreign-body and deep-thigh-wound mouse infection models. Antimicrob. Agents Chemother. **47:**2740–2748.
20. **Liang, J. J., C. L. Liao, J. T. Liao, Y. L. Lee, and Y. L. Lin.** 2009. A Japanese encephalitis virus vaccine candidate strain is attenuated by decreasing its interferon antagonistic ability. Vaccine **27:**2746–2754.
21. **Liang, P. H., M. Imamura, X. Li, D. Wu, M. Fujio, R. T. Guy, B. C. Wu, M. Tsuji, and C. H. Wong.** 2008. Quantitative microarray analysis of intact glycolipid-CD1d interaction and correlation with cell-based cytokine production. J. Am. Chem. Soc. **130:**12348–12354.
22. **Minagawa, S., C. Ohyama, S. Hatakeyama, N. Tsuchiya, T. Kato, and T. Habuchi.** 2005. Activation of natural killer T cells by alpha-galactosylceramide mediates clearance of bacteria in murine urinary tract infection. J. Urol. **173:**2171–2174.

23. **Morita, M., K. Motoki, K. Akimoto, T. Natori, T. Sakai, E. Sawa, K. Yamaji, Y. Koezuka, E. Kobayashi, and H. Fukushima.** 1995. Structure-activity relationship of alpha-galactosylceramides against B16-bearing mice. J. Med. Chem. **38:**2176–2187.

24. **Natori, T., M. Morita, K. Akimoto, and Y. Koezuka.** 1994. Agelasphins, novel antitumor and immunostimulatory cerebrosides from the marine sponge Agelas mauritianus. Tetrahedron **50:**2771–2784.

25. **Sireci, G., M. P. La Manna, D. Di Liberto, M. Lo Dico, M. Taniguchi, F. Dieli, and A. Salerno.** 2008. Prophylaxis of lipopolysaccharide-induced shock by alpha-galactosylceramide. J. Leukoc. Biol. **84:**550–560.

26. **Sireci, G., M. P. La Manna, C. Di Sano, D. Di Liberto, S. A. Porcelli, M. Kronenberg, F. Dieli, and A. Salerno.** 2007. Pivotal advance: alpha-galactosylceramide induces protection against lipopolysaccharide-induced shock. J. Leukoc. Biol. **81:**607–622.

27. **Su, C. Y., S. Y. Wang, J. J. Shie, K. S. Jeng, N. J. Temperton, J. M. Fang, C. H. Wong, and Y. S. Cheng.** 2008. In vitro evaluation of neuraminidase inhibitors using the neuraminidase-dependent release assay of hemagglutinin-pseudotyped viruses. Antiviral Res. **79:**199–205.

28. **Taniguchi, M., M. Harada, S. Kojo, T. Nakayama, and H. Wakao.** 2003. The regulatory role of Valpha14 NKT cells in innate and acquired immune response. Annu. Rev. Immunol. **21:**483–513.

29. **Thurnhofer, S., and W. Vetter.** 2007. Synthesis of (S)-(+)-enantiomers of food-relevant (n-5)-monoenoic and saturated anteiso-fatty acids by a Wittig reaction. Tetrahedron **63:**1140–1145.

30. **Trappeniers, M., S. Goormans, K. Van Beneden, T. Decruy, B. Linclau, A. Al-Shamkhani, T. Elliott, C. Ottensmeier, J. M. Werner, D. Elewaut, and S. Van Calenbergh.** 2008. Synthesis and in vitro evaluation of alpha-GalCer epimers. Chem. Med. Chem. **3:**1061–1070.

31. **Tupin, E., Y. Kinjo, and M. Kronenberg.** 2007. The unique role of natural killer T cells in the response to microorganisms. Nat. Rev. Microbiol. **5:**405–417.

32. **van der Vliet, H. J., J. W. Molling, B. M. von Blomberg, N. Nishi, W. Kolgen, A. J. van den Eertwegh, H. M. Pinedo, G. Giaccone, and R. J. Scheper.** 2004. The immunoregulatory role of CD1d-restricted natural killer T cells in disease. Clin. Immunol. **112:**8–23.

33. **van Dommelen, S. L., H. A. Tabarias, M. J. Smyth, and M. A. Degli-Esposti.** 2003. Activation of natural killer (NK) T cells during murine cytomegalovirus infection enhances the antiviral response mediated by NK cells. J. Virol. **77:**1877–1884.

34. **Velmourougane, G., R. Raju, G. Bricard, J. S. Im, G. S. Besra, S. A. Porcelli, and A. R. Howell.** 2009. Synthesis and evaluation of an acyl-chain unsaturated analog of the Th2 biasing, immunostimulatory glycolipid, OCH. Bioorg. Med. Chem. Lett. **19:**3386–3388.

35. **Wu, D., M. Fujio, and C. H. Wong.** 2008. Glycolipids as immunostimulating agents. Bioorg. Med. Chem. **16:**1073–1083.

36. **Wu, D., D. M. Zajonc, M. Fujio, B. A. Sullivan, Y. Kinjo, M. Kronenberg, I. A. Wilson, and C. H. Wong.** 2006. Design of natural killer T cell activators: structure and function of a microbial glycosphingolipid bound to mouse CD1d. Proc. Natl. Acad. Sci. U. S. A. **103:**3972–3977.

37. **Wu, L., and L. Van Kaer.** 2009. Natural killer T cells and autoimmune disease. Curr. Mol. Med. **9:**4–14.

38. **Wu, S. F., C. J. Lee, C. L. Liao, R. A. Dwek, N. Zitzmann, and Y. L. Lin.** 2002. Antiviral effects of an iminosugar derivative on flavivirus infections. J. Virol. **76:**3596–3604.

39. **Yoshimoto, T., A. Bendelac, C. Watson, J. Hu-Li, and W. E. Paul.** 1995. Role of NK1.1+ T cells in a TH2 response and in immunoglobulin E production. Science **270:**1845–1847.